Journal of Engineering and Applied Research (JEAR)

National University of Skills

Summer & Autumn 2025, Vol. 2, No. 2, p. 64- 85

Journal Homepage: https://jear.tvu.ac.ir

:10.48301/JEAR.2024.474745.1064

Effect of Electroslag Welding on the Mechanical Properties of Beam-column Connection of St52 Steel Structures

Moslem Mohammadi Soleymani[1], Aliakbar Majidi Jirandehi[2*]

[1,2] Mechanical Engineering Department, Payame Noor University, Tehran, Iran.

ARTICLE INFO

Article Type:
Original Research

Received: 02.06.2025
Revised: 05.15.2025
Accepted: 06.09.2025

Keyword:
Beam-to-column connectio
Electroslag welding (ESW)
Steel structures
Mechanical properties
St52 Steel

***Corresponding Author:**
Aliakbar Majidi Jirandehi
Email:
Aliakbar.majidi@PNU.ac.ir

ABSTRACT

In the metal structure industry, electroslag welding (ESW) is widely recognized as an effective method for joining thick sections, particularly in building box constructions and column stiffener assemblies. This study examines ST52 steel due to its widespread industrial applications and the lack of prior research investigating its mechanical properties when welded using the electroslag welding (ESW) technique. Two 20 mm thick St52 steel plates were joined via ESW at welding currents of 200 A and 250 A to simulate a beam-to-column connection. The welded joints were evaluated for hardness, impact resistance, tensile strength, and bending properties. Hardness testing revealed an inverse relationship between heat input and weld metal hardness, while the heat-affected zone (HAZ) exhibited increased hardness relative to the base St52 steel. The average impact energy of the St52 steel (81J) was found to be lower than the average impact energy of the weld metal. As the heat input increases, the grains get coarser, causing cavities to develop on the fracture surfaces and a reduction in fracture energy. The tensile sample fractured at the St52 base metal because the ultimate strength of the St52 steel connection in both samples exceeded 480 MPa. In light of the tensile and bending test findings, the ESW process was approved in full for joining the beam to the column. No defect was found that would compromise the mechanical properties of the weld.

E-ISSN: 3060-6357

Introduction

High-strength steels are widely employed in various industries, particularly in steel structure construction, due to their exceptional mechanical properties and weldability. Consequently, welding these steels is essential in large-scale projects. Given the substantial dimensions of the assembled structures, high heat input welding is often required [1;2].

The welding process influences the microstructure of the weld in the joints, which in turn affects the size of the heat-affected zone (HAZ) and the residual stresses on the base metal; in addition to the mechanical considerations related to the design of the connections, the welding process, filler materials, heat input, the number of weld passes, etc. [3]. The strength of the structure for structural steels is determined by the strength of the welded joints. Welding plays a significant role in extending the fatigue life of structural components because welded joints are exposed to cyclic loads in real-world applications and experience fatigue. The assessment of welded joints in industry is a significant issue for two primary reasons. The first is that because of poor material properties and the effects of stress concentration, the weld in a structure is often the weakest point. The second is that, it is hard to forecast their behavior with any degree of accuracy. The challenge of characterizing the material properties, which vary throughout the weld and the HAZ, contributes to this in part [4].

All codes and standards (AWS D1.1, ASME, API) recognize and approve the electroslag welding (ESW) process, which is utilized in metal structures, machinery, shipbuilding, rail and railway industries, casting, and bridge construction. When compared to other welding techniques, ESW is the most economical and dependable kind of welding for connecting thick connections with a diameter of up to 150 mm [5]. This kind of welding is used to unite exceptionally thick parts in a vertical or almost vertical position in a single pass. It is useful for welding inaccessible portions that are challenging or impossible to weld using traditional arc welding techniques.

The process starts when an electric arc forms between the joint groove's end and the electrode wire's tip. The flux (powder) is melted by the electric arc's heat. The electric arc is swiftly put out, causing a layer of molten slag to develop and directing the welding current from the electrode into the molten slag. The electrical resistance of the molten slag, which the welding current travels through, produces the heat needed for welding. As the welding process continues, the molten metal that is created from the base metal and the consumable wire rises and solidifies. This process proceeds continually until

the weld metal fills the whole joint area. The liquid weld metal is always present on top of the solid weld metal, with molten slag on top of both [5].

Researchers have paid particular attention to examining the seismic behavior of steel buildings since the 1995 Hanshin-Awaji earthquake [6]. In contrast to previous standards, current design guidelines highlight the need for increased toughness in beam-to-column connections. For these kinds of connections, toughness in Japan must be at least 70 Joules of Charpy absorbed energy at 0 degrees Celsius [7;8]. The correlations between heat input, inter-pass temperature, and Charpy absorbed energy in conventional welded connections have been the subject of numerous studies in the field of welding, and the findings have been reported in extensive databases [9]. Recently, Kojima et al. [7] established a formula based on the chemical composition of the steel in electroslag welded box-section columns to predict the toughness of the HAZ. The researchers were able to adjust the $\Delta t_{8/5}$ time for the HAZ in the range of 300 to 600 seconds through the use of a thermal simulator to reproduce the thermal cycles caused by the ESW process.

The diaphragm plates and column plates are joined using the ESW method to achieve maximum productivity [10]. However, because the ESW process requires a lot more heat than other fusion welding techniques like gas metal arc welding (GMAW) and shielded metal arc welding (SMAW), it frequently reduces the mechanical properties of the welded joint, especially its fracture toughness [6; 10]. Consequently, it can be concluded that the safety of the welded structure may be considerably impacted by the changes in material properties brought about by the ESW process. Eq. (1) defines the heat input H, which is the amount of energy produced per unit length of welding [11].

$$H = \frac{EI}{V} \tag{1}$$

Where E is the electric potential (V), I implies the electric current (A), and V denotes welding speed (wire consumption rate).

To improve the mechanical properties of the weld joints generated by the ESW method, researchers have studied how to optimize the parameters of the process with the aim of limiting the size of the Heat Affected Zone (HAZ). Through the use of low-basicity slag and wire containing Ti-B, Kitani et al. [12] were able to establish a totally acicular ferritic microstructure in the weld metal, hence improving the toughness of the fusion zone. In order to attain high tensile strength, Kojima et al. [7] studied how to manage the $\Delta t_{8/5}$ of the HAZ area within a reasonable range. On the other hand, not much study has been done on how using fast cooling methods like water and copper cooling may shorten the $\Delta t_{8/5}$ and ΔtH in the ESW process and reduce the HAZ size.

Theoretically, $\Delta t_{8/5}$ and ΔtH should both shorten throughout the ESW process when fast cooling techniques are used, and the HAZ region's size should also decrease somewhat. The fracture toughness of the ESW welds may be greatly increased after the effective use of quick cooling techniques in the welding process. The finite element method-based numerical simulation has also been extensively used in the computation of residual stresses, welding deformation, heat cycles, and even the microstructure and hardness of the material [6;13]. The microstructural and mechanical properties of friction-stir welded aluminum sheets were analyzed, revealing that grain refinement enhances mechanical properties, while tool pin profile and process parameters significantly affect defect formation and hardness distribution [14]. The tensile strength of friction-stir welded polypropylene sheets was analyzed, showing that tool geometry and welding angle significantly impact strength, with the highest tensile strength observed at a machine angle of 2 degrees [15].

The research investigates the fracture behavior of ESW joints in 590-N/mm^2 class steel using numerical analysis and finite element analysis with the fracture criterion, exploring material-scale characteristics, structural-scale behavior, and implications for higher-grade steel guidelines [16]. The novel 3-wire (ESW) technique effectively joins high-speed pearlite railway steel, producing defect-free joints and uniform mechanical properties. This is achieved through optimized heat generation and microstructure refinement, resulting in high hardness, tensile strength, and toughness in both weld metal and the HAZ [17].

Since the metal ST52 has many uses in industry and its mechanical properties have not been investigated by ESW, it has been considered in this study. The mechanical properties of welds in steel structures were examined in this study as a result of ESW. An analysis was conducted to analyze the mechanical properties of various weld regions and determine the ideal parameters for ESW in beam-to-column connections.

Materials and Methods

Material Selection

ST52 steel, a common material in metal building construction, was selected for this investigation. A 300 × 1500 × 20 mm ST52 steel plate (chemical composition detailed in Table 1) was welded using the electroslag welding (ESW) technique to complete the joint. The connection was made using the 3.2 mm-diameter AWS A5.17 EM12K electrode.

Table 1. Chemical composition of ST52 steel by weight percentage.

%C	%Mn	%P	%S	%Si

0.2	1.57	0.04	0.035	0.41

Electroslag Welding

The following devices, equipment, and materials were used in ESW. The parameters of ESW are given in Table 2.

1) ESW machine
2) AWS A5.17 EM12K electrode wire with a diameter of 3.2 mm with a chemical composition of 0.11% carbon, 0.18% silicon, and 1% manganese
3) AMA Universal slag flux equivalent to AWS A5.17 F7AZ
4) Elcoweld 610 nozzle
5) Construction steel sheet equivalent to ST52 standard

Table 2. Parameters of ESW.

Properties of Steel	Construction steel ST52
Welding process	Electroslag (ESW)
Reference standard	AWS D1.1
Welding condition	3G
Characteristics and class of electrode	AWS A5.17 EM12K_ES3.2 mm
Characteristics and class of flux	AWS A5.17 F7AZ (AMA Universal)
Characteristics and class of the nozzle	Elcoweld 610
Test plate thickness	20 mm
1 pass or multiple passes	1 pass
1 wire or multiple wires	1 wire
Flow type	Direct
Electrode polarity	Positive
Current (A)	Sample H1 with 200 A and sample H2 with 250 A
Potential difference (V)	35 V
Gap between two pieces	15 mm
Inner and outer diameter of the nozzle	Internal diameter: 4 mm

	External diameter: 10 mm

First, two steel plates with a thickness of 20 mm and dimensions of 150×300 mm were cut without any beveling. They were then assembled with a 15 mm gap using two 10 mm thick and 30 mm wide backing strips. One side of the gap between the two plates was sealed with a 10 mm thick plate, and the assembly was placed under the test setup. In this process, only one type of connection was used, which was a butt or tee joint with a square groove. The configuration of this joint is indicated in Figure 1 and 2.

The minimum distance between two workpieces is required for the following reasons:

- Sufficient slag formation
- Sufficient space for slag rotation
- Sufficient distance for the nozzle to pass

The large distance between two workpieces causes excessive electrode consumption, which is not cost-effective and also increases the possibility of non-melting defects.

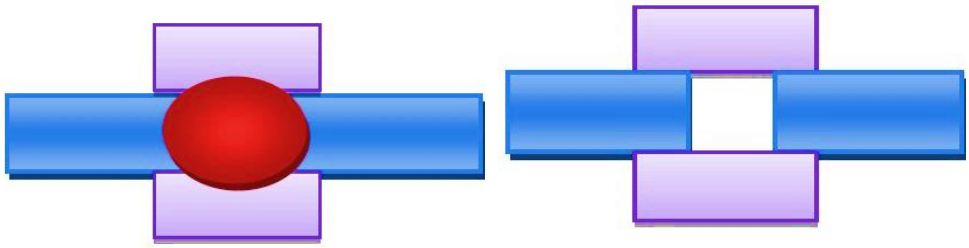

(a) (b)

Figure 1. ESW connection scheme, a) Before welding, b) After welding.

Figure 2. ESW plate test.

After installing the nozzle on the machine, passing the electrode through it, and ensuring the perpendicular alignment of the nozzle and electrode assembly using the machine's positioning and adjusting capabilities, the nozzle was guided all the way into the gap between the two plates (Figure 3). Using the default menu on the machine's panel, the selected current and voltage were adjusted to prepare the conditions for starting the welding process. The selected current and voltage values are presented in Table 2.

Figure 3. Way the part is placed for welding.

Before beginning the welding operation, around 50 grams of flux were injected into the space between the two plates. The backing plate was entirely red on both sides throughout the welding process, and there was little to no smoke or spattering. A small quantity of flux was manually supplied to the molten pool if a cracking noise and splatter were audible during the welding process. The workpiece was left outside to attain room temperature and be ready for both quantitative and qualitative assessments after the welding and gap filling were finished, which took around ten minutes. The workpiece underwent a radiographic test to verify the integrity of the weld. Defects, including porosity, trapped slag, fractures, or lack of fusion, were not seen during the radiography test. The HAZ, weld metal (WM), and base metal (BM) of the welded plates were subjected to a variety of mechanical testing. The cutting of a sample for the mechanical testing is illustrated in Figure 4.

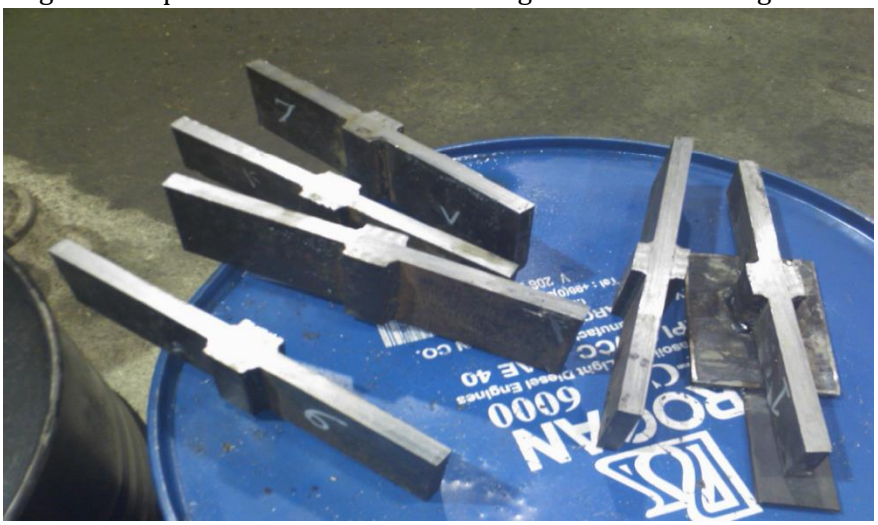

Figure 4. Cutting of the sample for mechanical tests.

Hardness Test

To examine the hardness variations in different regions of the St52 steel weld joint, the hardness was measured on the cross-section of the samples using a Vickers microhardness tester with a force of HV5 (49.03N), in accordance with the standard ISO 6507-1:2005. Figure 5 is a schematic of the joint configuration and the hardness measurement points.

.

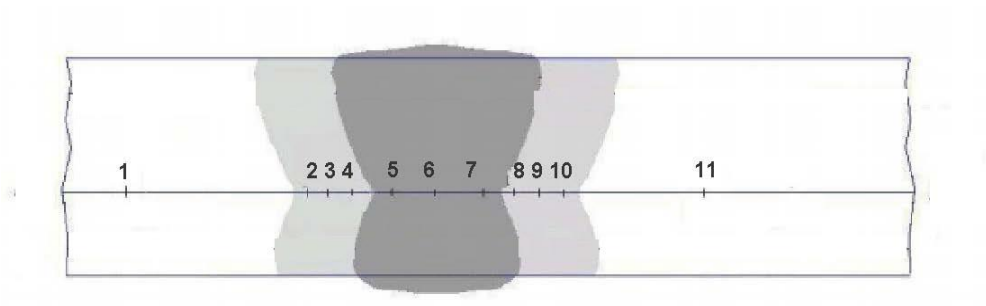

Figure 5. Schematic of joint configuration and the hardness measurement points.

Impact Test

The ASTM E23 (2016) standard was followed for conducting the Charpy impact test at room temperature on both the base and weld metal. A schematic representation of the joint structure and the impact test sample locations is presented in Figure 6, where the notches are located in the areas of the base metal and the weld metal. The impact test samples' dimensions are shown in Figure 7. The notches on the samples were cut perpendicular to the weld line at a depth of two millimeters from the plate's surface. An impact testing device called the SANTAM SIT-300 was used to conduct the tests. For every sample, three Charpy impact tests were performed, and the average absorbed energy from the three tests was calculated.

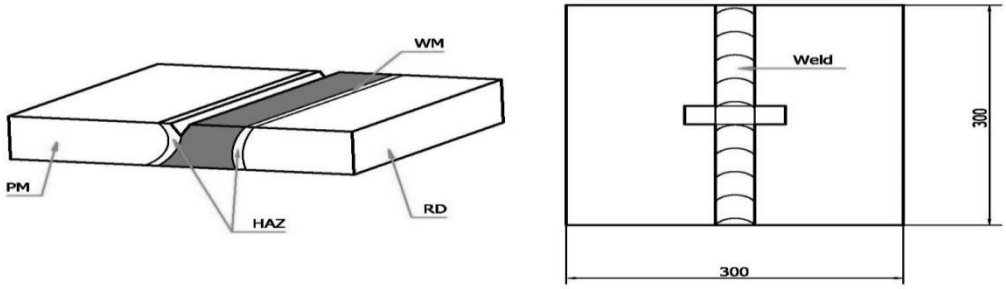

Figure 6. Schematic illustration of the connection scheme and the position of the impact samples.

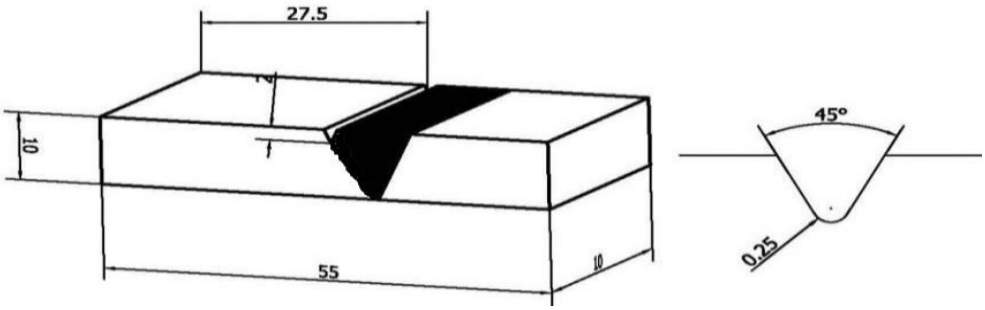

Figure 7. Dimensions of the tested impact samples.

Tensile Test

The purpose of the tensile test was to evaluate the samples' ultimate tensile strength and yield strength as a result of the room-temperature welding procedure. It was decided to cut the tensile test samples perpendicular to the weld line. An English-made INSTRON type 4208 universal testing equipment with a 30-ton capacity was used to perform the tensile test in accordance with ASME guidelines. For each joint, two transverse tensile test samples were considered. The schematic and dimensions of the tensile test samples are shown in Figure 8.

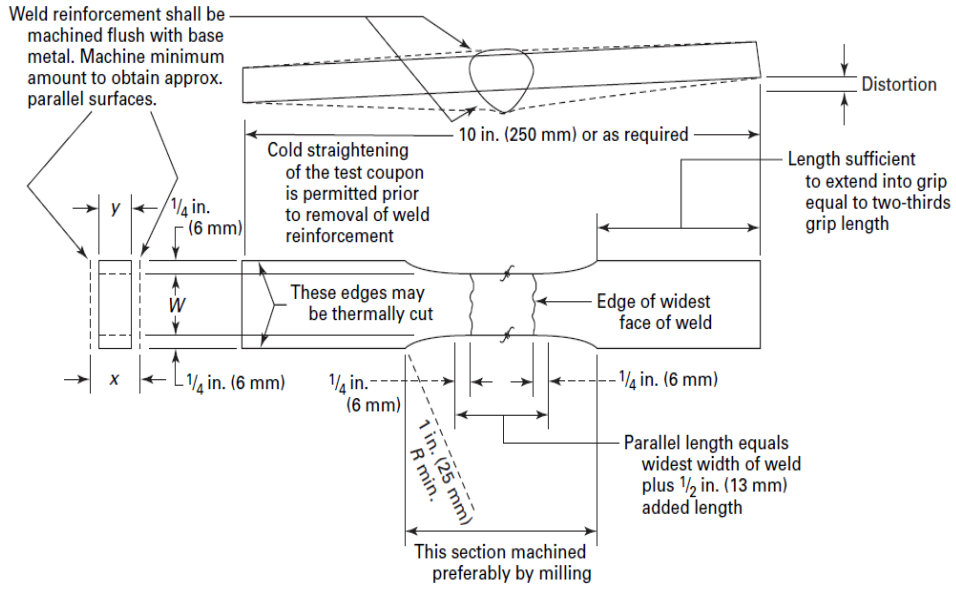

Figure 8. Schematic illustration and dimensions of transverse tensile weld samples [22].

The following are the tensile test acceptance requirements as stated in the ASME standard: the minimal ultimate tensile strength required for the base metal should not be less than the ultimate tensile strength that is achieved. The test is deemed satisfactory if the test sample breaks outside the weld line. Nevertheless, the tensile strength must not fall below 95% of the base metal's minimum ultimate tensile strength [18].

Bending test

In this study, a 3-point bending test according to the ASME standard was used. Every welded plate underwent two 180-degree face bends and two 180-degree root bends as part of the bending tests carried out in compliance with the ASME standard. The following is the ASME standard acceptance criteria for the bending test:

Surface discontinuities larger than 3.2 millimeters in any direction on the external (convex) surface of the sample after bending in the weld metal or HAZ are not acceptable. Surface discontinuities that occur at the corners of the sample during the test can be ignored unless the discontinuities are caused by incomplete fusion or entrapped slag inclusions in the weld or other internal defects [18].

Results and Discussion

Hardness Measurement Results

Vickers hardness testing was performed to evaluate hardness distribution across the St52 steel electroslag weld. As presented in Tables 3 and 4, the hardness measurements were taken from cross-sections of ESW-welded components. Hardness profiles comparing the base metal (St52), heat-affected zone (HAZ), and weld metal were generated (Figure 9), revealing significant variations in microhardness across these regions.

The HAZ on both sides of the St52 steel joint has become harder, according to the hardness data shown in Figure 9. This is because the coarse-grained microstructure gradually replaces the fine-grained microstructure in the HAZ close to the weld metal, and the hardness of this area drops as the welding process's heat input increases [19]. To be more precise, sample H1, which had the lowest heat input, has the maximum hardness in the HAZ, while sample H2, which had the highest heat input, has the lowest hardness.

Table 3. Hardness measurement results of welding connection of St52 steel with ESW method.

Hardness testing position	Vickers hardness (HV)	
	Sample H1 Current 200 Amps	Sample H2 Current 250 Amps
Base (1)	135	134
HAZ (2)	150	135
HAZ (3)	159	151
HAZ (4)	160	150
Weld (5)	206	180
Weld (5)	209	213
Weld (7)	206	207
HAZ (8)	152	148
HAZ (9)	150	156
HAZ (10)	152	152
Base (11)	134	134

Table 4. Average hardness of St52 steel weld joint in different welding currents.

Sample	Average weld hardness (HV)	Average HAZ hardness (HV)	Average base hardness (HV)
Sample H1 Current 200 Amps	207	154	135
Sample H2 Current 250 Amps	200	148.7	134

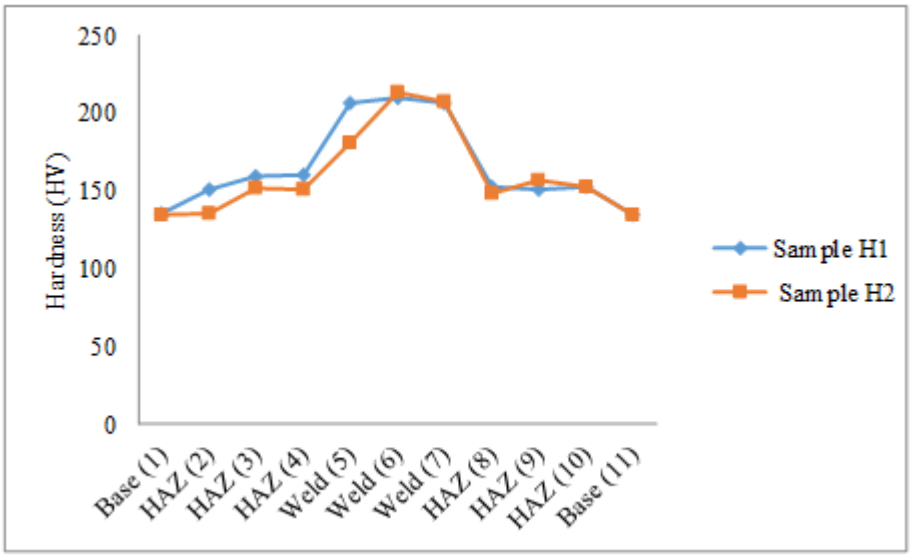

Figure 9. Vickers hardness changes of St52 steel joint in different welding currents.

The hardness of the various weld zones diminishes, according to the hardness data for sample H2 shown in Figure 9. Since more heat was delivered to this area during the welding process, the crucial HAZ of the weld showed the lowest hardness when compared to the other sample. The hardness variance throughout the weld areas in the three samples with varying heat inputs is shown by the average hardness values in the various weld positions for samples H1 and H2, presented in Table 4. This indicates a predominance of heterogeneous microstructures in the various weld regions. Furthermore, the average Vickers hardness values of the HAZ and base metal exhibit comparable behavior to that of the weld metal in the two distinct samples. On both sides of the weld joint, the average HAZ hardness was greater than that of the base metal. When compared to the other samples, Sample H1 showed the greatest HAZ hardness. A result of the increased heat input from the welding operation carried out on both sides of the samples, the hardness of the HAZ in the H2 samples has decreased. High heat input welding techniques, such as submerged arc and ESW, are often used for welding steel structures. However, these welding techniques slow down the rate at which the HAZ areas cool down, which causes grain formation in the microstructure and worsens the HAZ's characteristics, including its hardness [20;21].

An increase in welding heat input precludes the creation of high-hardness structures, according to research on the impact of welding heat input on the microstructure and mechanical properties of the HAZ in high-strength, low-alloy steel joints. In comparison to the base metal, the Vickers hardness of structural steel joints is significantly higher in the HAZ and fusion zone (FZ). As welding heat input increases, the average HAZ hardness drops. The coarse-grained zone has a harder structure than the fine-grained region when less welding heat is applied [22].

Table 4 indicates that sample H1's weld metal has the maximum hardness, while sample H2's weld metal has the lowest hardness. This is because when welding heat input increases, the weld metal's hardness falls. This is because applying more welding heat input causes a change in the morphology of the weld metal structure. The cooling rate decreases as heat input increases, enabling the weld to remain at greater temperatures for extended periods of time. The resultant coarse grains will cause the hardness to decrease [23].

Impact Test Results

Impact tests were conducted at room temperature on the St52 base metal and the 200 A and 250 A electroslag weld metal at welding currents. Table 5 presents the impact test results for the samples that were welded using various welding currents. The weld metal samples have higher impact energies than the St52 steel sample, as indicated by the impact test results shown in Table 5 and Figure 10. This increase in impact energy of the weld metal in the St52 steel joint by employing ESW can be attributed to the homogeneous microstructure of the weld metal.

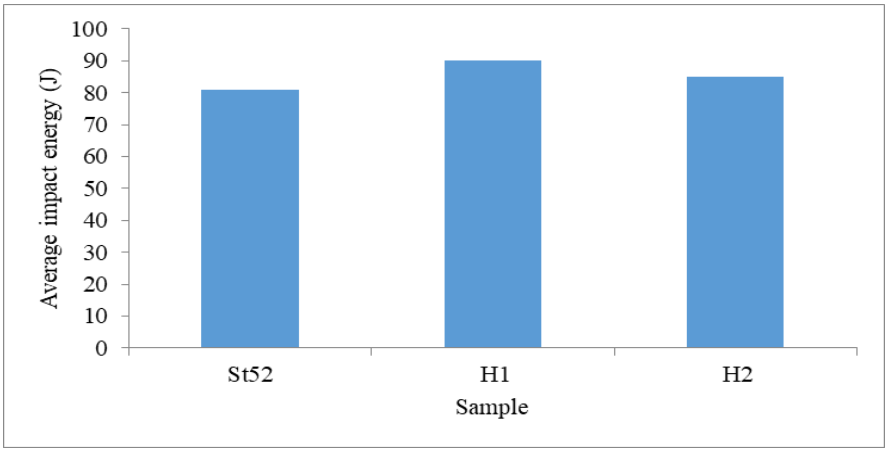

Figure 10. Bar chart of the average impact energy of the base metal and weld in different welding currents.

Table 5. Results of impact test of samples at ambient temperature.

Sample	Notch position	Impact energy (J)	Average impact energy (J)
Sample base ST52	Base	91	81
		69	
		83	
Sample H1 Current 200 Amps	Weld	86	90
		93	
		91	
Sample H2 Current 250 Amps	Weld	95	85
		70	
		90	

Table 5 shows the impact energy of the St52 steel joint at welding currents of 200 A and 250 A. Sample H1 and H2 have the highest and lowest impact energies, respectively. As a result, as shown in Table 5 and Figure 10, the weld metal's impact toughness is greater than the base metal's for each sample. The fracture energy falls as the heat input increases because the coarsening of the grains and the development of a coarse structure occur from this process. Cracks at grain boundaries might spread more readily as the grains expand. Increased heat input may also result in a higher proportion of precipitates, which may function as a source of fractures and lower fracture energy as a result. One of the primary causes of a decrease in toughness is the coarse structure. The toughness of the HAZ and the weld metal is often reduced in the presence of a coarse structure. The constituents present in the structure also play a crucial role in the toughness or brittleness of the HAZ and the weld metal. Overall, a fine-grained structure is a good microstructure for toughness [20;21].

Tensile Test Results

Tensile tests were conducted at room temperature according to the ASME SEC IX standard, and the transverse cross-sectional type of the weld region was considered. The results of the tensile tests are presented in Table 6.

Table 6. Tensile test results of ESW samples.

Sample	Fracture area	Ultimate strength (N/mm2)	Yield strength (N/mm2)	Thickness×Width (mm×mm)	Cross-sectional area (mm2)
H1-T1	HAZ	527	456	19.04×5.92	112.72
H1-T2	HAZ	523	444	19.02×5.92	112.59
H2-T1	HAZ	502	410	19.07×6.25	119.18
H2-T2	HAZ	480	421	19.08×6.25	119.25

Since the thickness of the T1 samples is equal to each other, and the thicknesses of the T2 samples are also the same, it does not create a problem for conducting the test and analyzing the results. According to the ASME IX standard [18], the minimum acceptable tensile strength for transverse samples in relation to the weld line for St52 steel is equal to 455 MPa. Considering the results obtained from the tensile tests, both welded samples exhibited a final strength higher than the permissible limit in the ASME standard. The weld strength of both samples was higher than the St52 base metal so that the tensile test sample failed from the HAZ of the base metal. One may infer that there are no faults that might compromise the mechanical properties of the weld and that the weld quality is entirely approved with regard to weld soundness. The transverse weld test samples of H1 and H2, which were welded via the ESW technique with currents of 200 A and 250 A, respectively, are compared in Figures 11 and 12.

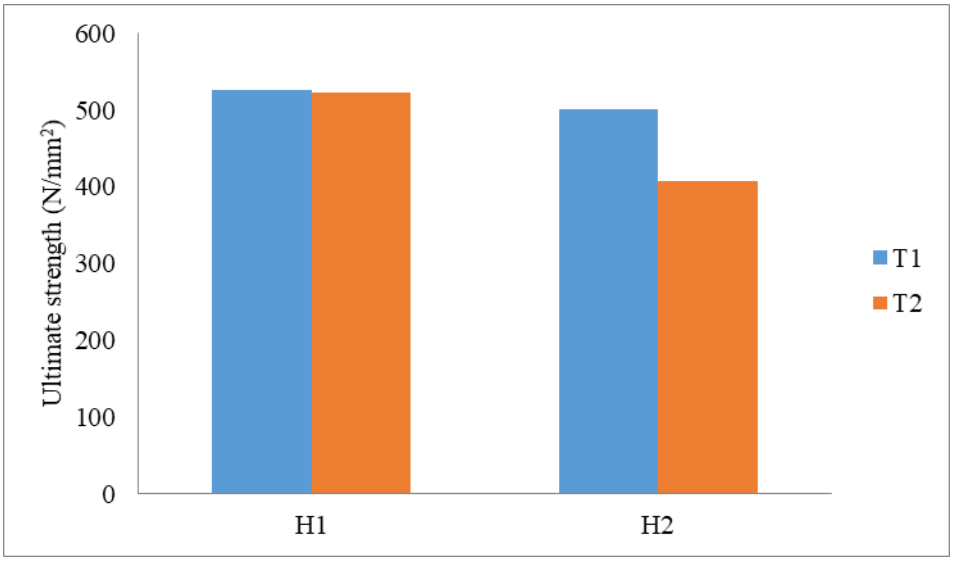

Figure 11. Comparison of final strength of samples welded by electroslag method.

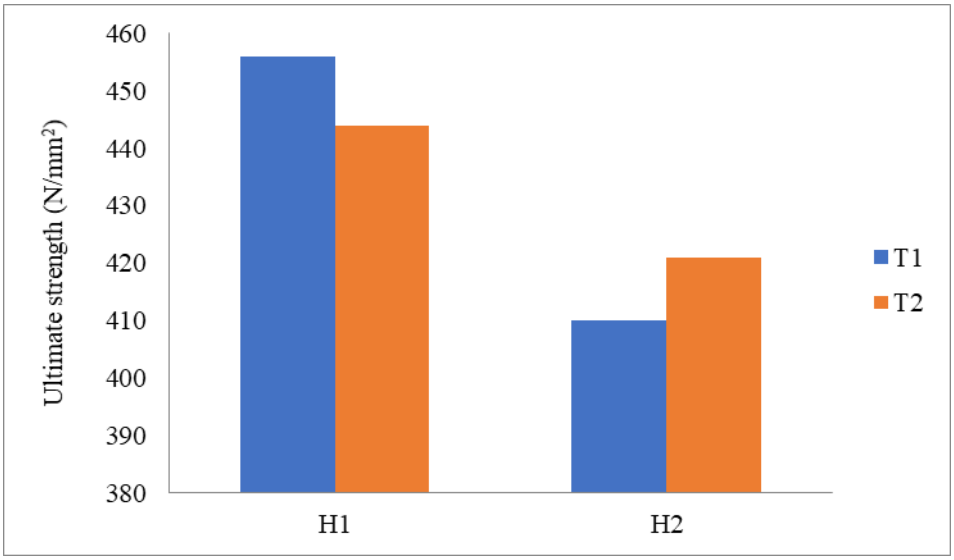

Figure 12. Comparison of yield strength of samples welded by electroslag method.

According to the tensile test results, sample H1 welded with a current of 200 A has a higher ultimate and yield strength compared to sample H2 welded with 250 A, indicating that the size of the HAZ in sample H2 is considerably larger than that of sample H1. The weld fusion line typically reaches a maximum

temperature of 1500°C, and the HAZ usually has a temperature between 700 to 1500°C [10;24]. The St52 steel joint in the 250 A welded sample has lower strength compared to the 200 A sample, which can be attributed to the weakening of the HAZ due to the thermal welding cycle. Consequently, in order to achieve the appropriate mechanical properties for the St52 steel joint during the ESW process, it is advised to utilize a lower welding current. This is because a higher welding current increases the heat input, which causes the HAZ to expand. The transverse weld tensile test samples' fracture position is shown in Figure 13.

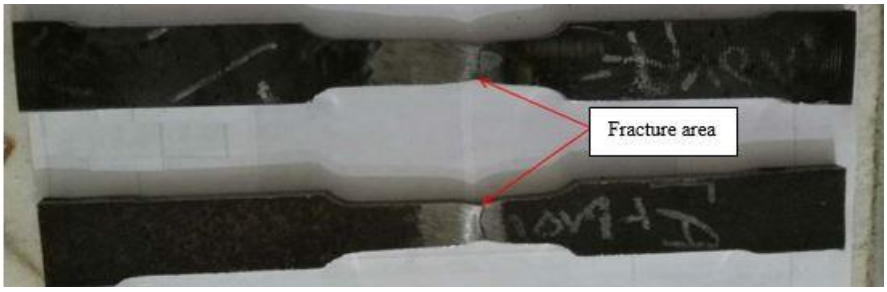

(a)

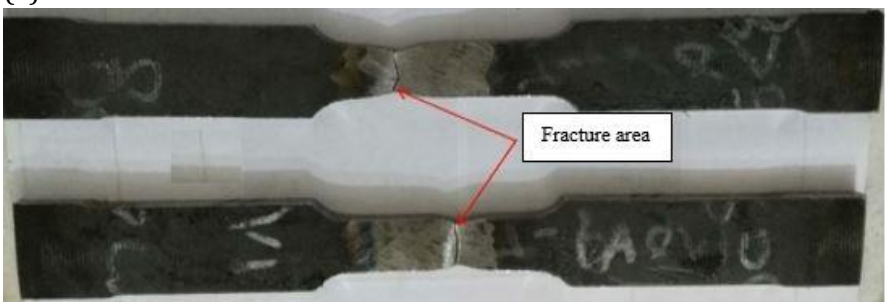

(b)

Figure 13. Fracture region of the transverse tensile weld samples, a) Samples H1, b) Samples H2.

Bending Test Results

The results regarding the ESW bending tests are presented in Tables 7 and 8. The results of the 180-degree bending test for the WSW samples were obtained from 3-point bending test samples. After visual inspection of the sample surfaces, no discontinuities outside the standard acceptance limits were observed in any of the samples. Figure 18 presents the images of the bending samples after the test.

Table 7. Bending test results of electroslag welded sample H1.

number	Thickness (mm)	Mandrel diameter (mm)	Bending angle	Test result
1	15.60	38	180	Without fault
2	15.65	38	180	Without fault

Table 8. Bending test results of electroslag welded sample H2.

number	Thickness (mm)	Mandrel diameter (mm)	Bending angle	Test result
1	15.55	38	180	Without fault
2	15.45	38	180	Without fault

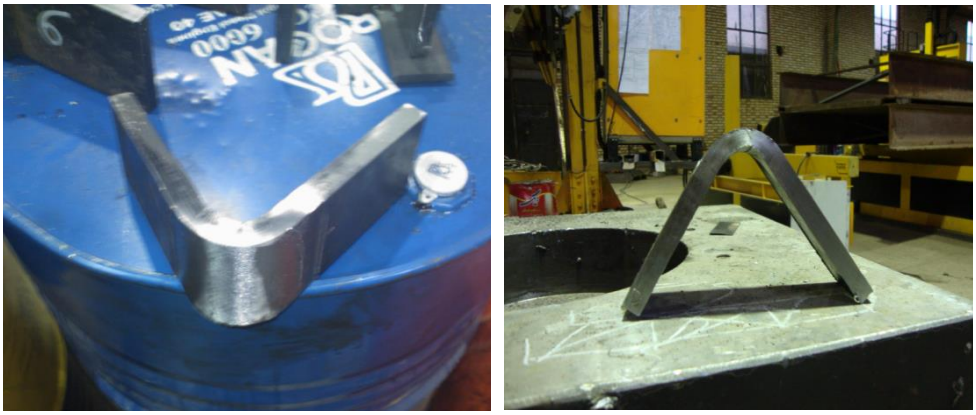

Figure 18. Images of the samples after the bending test

Conclusion

Two St52 steel joint samples were created for this investigation utilizing the ESW method under various heat input conditions. Two samples were welded: sample H1 was welded at 200 A, while sample H2 was welded at 250 A. After evaluating the welds' hardness, impact resistance, tensile behavior, and bending behavior, the following conclusions can be drawn:

- Compared to the base St52 steel, the hardness of the heat-affected zone (HAZ) increased. However, increasing the welding heat input led to a reduction in weld metal hardness.
- The weld metal exhibited higher impact energy than the base St52 steel, with averages of 90 J for sample H1 and 85 J for sample H2, compared to 81 J for the base material. However, increased heat input led to grain coarsening, which promoted cavity formation on fracture surfaces and consequently reduced fracture energy.
- The tensile test results for the two electroslag welded samples indicate that the weld strength is greater than 480 MPa. Taking into account that the ASME standard specifies 455 MPa as the minimum acceptable strength for welded St52 steel sections, it is possible to conclude that the weld quality is fully approved in terms of weld soundness.
- In addition, the tensile test findings indicate that the weld's strength exceeds that of the base metal, which is why the tensile sample failed where the base metal was. As a result, in terms of weld soundness, the ESW process is completely approved for connecting the beam to the column.
- The bending test results confirm that the weld exhibits no defects compromising its mechanical properties, fully meeting quality standards for weld soundness.

Disclosure statement and funding

The authors declare no potential conflicts of interest. The present study received no financial support from any organization or institution.

References

[1] Xue, Q., Benson, D., Meyers, M., Nesterenko, V., & Olevsky, E. (2003). Constitutive response of welded HSLA 100 steel. *Materials Science and Engineering: A*, *354*(1-2), 166-179. https://doi.org/10.1016/S0921-5093(03)00007-8

[2] Harada, Y., Iyama, J., Matsumoto, Y., & Oki, K. (2023). Electroslag Welding Applications for Steel Building Construction in Japan: A State-of-the-Art Review. *Engineering Journal*, *60*(2), 93-110. https://doi.org/10.62913/engj.v60i2.1201

[3] Ion, J. C., & Easterling, K. E. (1985). Computer modelling of weld-implant testing. *Materials science and technology*, *1*(5), 405-411. https://doi.org/10.1179/mst.1985.1.5.405

[4] Taylor, D., Barrett, N., & Lucano, G. (2002). Some new methods for predicting fatigue in welded joints. *International Journal of Fatigue*, *24*(5), 509-518. https://doi.org/10.1016/S0142-1123(01)00174-8

[5] Bong, W. L. (2012). *U.S. Patent No. 8,110,772* (Washington, DC: U.S. Patent and Trademark Office Patent No.

[6] Deng, D., & Kiyoshima, S. (2012). Numerical simulation of welding temperature field, residual stress and deformation induced by electro slag welding. *Computational materials science*, *62*, 23-34. https://doi.org/10.1016/j.commatsci.2012.04.037

[7] Kojima, A., Yoshii, K.-I., Hada, T., Saeki, O., Ichikawa, K., Yoshida, Y., Shimura, Y., & Azuma, K. (2004). Development of high HAZ toughness steel plates for box columns with high heat input welding. *Shinnittetsu Giho*, 33-37. https://www.nipponsteel.com/en/tech/report/nsc/pdf/n9009.pdf

[8] Kimura, T. (2005). High Tensile Strength Steel Plates and Welding Consumables for Architectural Construction with Excellent Toughness in Welded Joints-" JFE EWEL" Technology for Excellent Quality in Large Heat Input Welded Joints. *JFE technical report*, *5*, 45-52. https://cir.nii.ac.jp/crid/1571698600739586688

[9] Hashiba, Y., Hasegawa, T., Ohkita, S., Yoshida, Y., & Shimura, Y. (2007). Metallurgical Controlling Factors for Toughness of Multi-layered Weld Metal in Beam-to-column Connections. *Nippon Steel Technical Report No*, *95*. https://www.nipponsteel.com/en/tech/report/nsc/pdf/n9513.pdf

[10] Chen, C.-C., & Liang, Y.-C. (2011). The effects of electro slag welding on material properties of box column plates. *International Journal of Steel Structures*, *11*(2), 171-189. https://doi.org/10.1007/s13296-011-2006-2

[11] Debroy, T., Szekely, J., & Eagar, T. (1980). Heat generation patterns and temperature profiles in electroslag welding. *Metallurgical Transactions B*, *11*(4), 593-605. https://doi.org/10.1007/BF02670139

[12] Kitani, Y., Ikeda, R., Ono, M., & Ikeuchi, K. (2009). Improvement of weld metal toughness in high heat input electro-slag welding of low carbon steel. *Welding in the World*, *53*(3), R57-R63. https://doi.org/10.1007/BF03266704

[13] Ueda, Y., Murakawa, H., & Ma, N. (2007). Computational approach to welding deformation and residual stress. *Sanpo Publication*.

[14] Akbari, M., & Asadi, P. (2022). Experimental Investigation of Welding Defects in Butt Joining of Aluminum Alloy by Friction Stir Welding: Effects of Tool Pin Profile and Process Parameters. *Karafan Quarterly Scientific Journal*, *19*(1), 125-143. https://doi.org/10.48301/kssa.2021.285680.1523

[15] Asadi Boroojeni, B., & Mozafari Vanani, L. (2020). The effect of tool geometry on the tensile strength of polypropylene Components Welded by Friction Stir Welding Method. *Karafan Journal*, *17*(1), 133-145. https://doi.org/10.48301/kssa.2020.112761

[16] Li, H., & Iyama, J. (2024). Investigation on Fracture Behavior of Electroslag Welding Joint with High-Performance Steel. *International Journal of Steel Structures*, *24*(4), 882-891. https://doi.org/10.1007/s13296-024-00855-2

[17] Khan, A. R., & Shengfu, Y. (2025). Performance Evaluation of High Speed Pearlite Railway Steel Joint by 3-Wire Electroslag Welding. *Journal of Materials Engineering and Performance*, *34*(5), 4004-4014. https://doi.org/10.1007/s11665-024-09423-5

[18] Pressure, A. S. M. E. (2010). *Qualification Standard for Welding and Brazing Procedures, Welders, Brazers, and Welding and Brazing Operators*. American

Society of Mechanical Engineers. https://doi.org/https://doi.org/10.1115/1.802700

[19] Majidi-Jirandehi, A. A., Hashemi, S., Ebrahimi-Nejad, S., & Kheybari, M. (2021). Impact of crack propagation path and inclusion elements on fracture toughness and micro-surface characteristics of welded pipes in DWTT. *Materials Research Express*, *8*(10), 106504. https://doi.org/10.1088/2053-1591/ac2ae0

[20] Wan, X., Wu, K., Huang, G., & Wei, R. (2014). In Situ Observations of the Formation of Fine-Grained Mixed Microstructures of Acicular Ferrite and Bainite in the Simulated Coarse-Grained Heated-Affected Zone. *steel research international*, *85*(2), 243-250. https://doi.org/10.1002/srin.201200313

[21] Wan, X., Wei, R., & Wu, K. (2010). Effect of acicular ferrite formation on grain refinement in the coarse-grained region of heat-affected zone. *Materials Characterization*, *61*(7), 726-731. https://doi.org/10.1016/j.matchar.2010.04.004

[22] Dong, H., Hao, X., & Deng, D. (2014). Effect of welding heat input on microstructure and mechanical properties of HSLA steel joint. *Metallography, microstructure, and analysis*, *3*(2), 138-146. https://doi.org/10.1007/s13632-014-0130-z

[23] Lundin, C., Zhou, G., & Khan, K. (1995). Report Number 1: Metallurgical characterization of the HAZ in A516-70 and evaluation of fracture toughness specimens. *Bulletin-Welding Research Council*, *1*(403). https://www.osti.gov/biblio/109997

[24] Easterling, K. (2013). *Introduction to the physical metallurgy of welding*. Elsevier. https://books.google.com/books?hl=en&lr=&id=DfwkBQAAQBAJ&oi=fnd&pg=PP1&dq=Introduction+to+the+physical+metallurgy+of+welding&ots=fZEXMdgk15&sig=8KRus2mSpbfdH2p9ScGXx-9dHuU#v=onepage&q=Introduction%20to%20the%20physical%20metallurgy%20of%20welding&f=false